Research Square

Preprints are preliminary reports that have not undergone peer review.
They should not be considered conclusive, used to inform clinical practice,
or referenced by the media as validated information.

Exact Solutions and Dynamics of the Raman Soliton Model in Nanoscale Optical Waveguides, with Metamaterials, Having Anti-cubic Nonlinearity

Guoan Xu (xga99163@163.com)
Zhejiang Normal University https://orcid.org/0000-0002-9512-4406
Jibin Li
Huaqiao University
Yi Zhang
Zhejiang Normal University

Research Article

Keywords: Raman soliton model, anti-cubic, exact solution, solitary wave, peakon, periodic peakon, pseudo-peakon, compacton

Posted Date: May 10th, 2021

DOI: https://doi.org/10.21203/rs.3.rs-380510/v1

License: This work is licensed under a Creative Commons Attribution 4.0 International License.
Read Full License

Noname manuscript No.
(will be inserted by the editor)

Exact Solutions and Dynamical Behaviors of the Raman Soliton Model in Nanoscale Optical Waveguides, with Metamaterials, Having Anti-cubic Nonlinearity

Guoan Xu · Jibin Li · Yi Zhang

Received: date / Accepted: date

Abstract This paper investigates Raman soliton model in optical metamaterials, having anti-cubic nonlinearity. By travelling wave transformation, the model is transformed into a singular planar dynamical system having three singular straight lines. Using the bifurcation theory method of dynamical systems, under different parameter conditions, bifurcations of phase portraits are studied. More than 30 exact explicit solutions of planar dynamical system are derived, such as exact periodic wave solutions, solitary wave solutions, kink and anti-kink wave solutions, periodic peakons and peakons as well as compacton solutions. In more general parametric conditions, all possible solutions are found.

Keywords Raman soliton model · anti-cubic · exact solution · solitary wave · peakon · periodic peakon · pseudo-peakon · compacton

1 Introduction

The dynamic behavior of optical solitons is an important discovery in nonlinear optics. Many optical metamaterials with rich optical properties used to fabricate optical fibers have linear and nonlinear electromagnetic properties. The Raman soliton model describes the phenomenon of optical solitons generated during the propagation of optical waves in optical metamaterials. This model has aroused a great deal of research interest among scholars [1-9].

Xiang et al.[2] derived and gave the non-linear Schröinger's (NLSE) equation of Raman soliton propagation in optical metamaterials by Maxwell

G. Xu · J. Li
School of Mathematical Sciences, Huaqiao University, Quanzhou 362021, China

G. Xu · J. Li · Y. Zhang(✉)
Department of Mathematics, Zhejiang Normal University , Jinhua 321004, China
E-mail: zy2836@163.com

equation

$$\begin{aligned} &iq_t + aq_{xx} + (c_1|q|^2 + c_2|q|^4 + c_3|q|^6)q \\ &= i\alpha q_x + i\lambda(|q|^2q)_x + i\nu(|q|^2)_xq + \theta_1(|q|^2q)_{xx} + \theta_2|q|^2q_{xx} + \theta_3q^2q^*_{xx}, \end{aligned} \tag{1}$$

where $a \neq 0, q(x,t)$ represents the complex-valued wave function, x and t represent spatial and temporal variables, respectively. α represents the coefficient of inter-modal dispersion. The factors λ and ν are considered to be self-steepening for preventing shock-waves, and non-linear dispersion. Finally, the terms with θ_j for $j = 1, 2, 3$ arise in the context of optical metamaterials. By using the bifurcation theory method of dynamical systems to the traveling wave system of equation (1), Zhou & Li [3] discussed the exact solutions and their dynamics.

More recently, Al-Ghafri & Krishnan [4] considered the following equation

$$\begin{aligned} &iq_t + aq_{xx} + (b_1|q|^{-4} + b_2|q|^2 + b_3|q|^4)q \\ &= i\alpha q_x + i\lambda(|q|^2q)_x + i\nu(|q|^2)_xq + \theta_1(|q|^2q)_{xx} + \theta_2|q|^2q_{xx} + \theta_3q^2q^*_{xx}. \end{aligned} \tag{2}$$

This model characterize the optical solitons in metamaterials dominated by anti-cubic nonlinearity. Eq. (2) has been studied by many scholars in order to obtain soliton solutions by several type of methods. Such as the generalized $\frac{G'}{G}$-expansion method [5],the extended trial equation method [6], the improved $\tan(\frac{1}{2}\phi(\xi))$-expansion method [7], three different integration schemes [8] and the Lie group method [9],etc.. In [4],under appropriate parametric conditions, the authors obtained the optical solitons and periodic wave solutions of equation (2) with the aid of four analytic methods, namely, the projective Riccati equations method[10], the new auxiliary equation method [11], the new mapping method [12] and the Bernoulli sub-ODE method [13]. However, there are still many other forms of solutions to Equation (2) and a large number of dynamic behaviors that have not been explored.

It is found that the solution of Eq. (2) has the following form

$$q(x,t) = \phi(\xi)\exp(i(-kx + \omega t)), \quad \xi = x - vt. \tag{3}$$

Substituting (3) into (2) and separating the real and imaginary part, we get

$$[a - (3\theta_1 + \theta_2 + \theta_3)\phi^2]\phi'' - a_1\phi + b_1\phi^{-3} + a_3\phi^3 + b_3\phi^5 - 6\theta_1\phi(\phi')^2 = 0, \tag{4_r}$$

$$(v + \alpha + 2ak) + [3\lambda + 2\nu - 2k(3\theta_1 + \theta_2 - \theta_3)]\phi^2 = 0, \tag{4_i}$$

where $a_1 = \omega + \alpha k + ak^2, a_3 = b_2 - k\lambda + (\theta_1 + \theta_2 + \theta_3)k^2$, the notation $\phi' = \frac{d\phi}{d\xi}$. From imaginary part Equation (4_i), set the coefficient of the linearly independent function to zero to obtain the following relations

$$v = -(\alpha + 2ak), \quad 3\lambda + 2\nu = 2k(3\theta_1 + \theta_2 - \theta_3). \tag{5}$$

Assume that $\theta_1 \neq 0$ and $3\theta_1 + \theta_2 + \theta_3 \neq 0$. Making the parameter transformation $a_0 = \frac{a}{3\theta_1+\theta_2+\theta_3}, \beta = \frac{3\theta_1+\theta_2+\theta_3}{6\theta_1}, g_0 = \frac{-b_1}{6\theta_1} \neq 0, \alpha_0 = \frac{a_1}{6\theta_1}, \alpha_2 =$

$-\frac{a_3}{6\theta_1}, \alpha_4 = -\frac{b_3}{6\theta_1}$ then, Equation (4_r) is equivalent to the following planar dynamical system

$$\frac{d\phi}{d\xi} = y, \quad \frac{dy}{d\xi} = \frac{\phi^4 y^2 + \phi^4(\alpha_0 + \alpha_2\phi^2 + \alpha_4\phi^4) + g_0}{\beta\phi^3(a_0 - \phi^2)}. \tag{6}$$

System (6) is an integrable planar dynamical system depending on the six-parameter group $(a_0, \beta, g_0, \alpha_0, \alpha_2, \alpha_4)$.

Remark 1 In [4], the authors assume that $\theta_1 = 0$ and $\theta_2 = -\theta_3$, i.e., $3\theta_1 + \theta_2 + \theta_3 = 0$. This is very special case in equation (4_r). In this case, system (6) reduces as follows

$$\frac{d\phi}{d\xi} = y, \quad \frac{dy}{d\xi} = \frac{\phi^4[(\omega + ak^2 + k\alpha) - (b_2 - k\lambda)\phi^2 - b_3\phi^4] - b_1}{a\phi^3}. \tag{7}$$

with the first integral

$$H_0(\phi, y) = \frac{1}{2}ay^2 - \frac{b_1}{2\phi^2} - \frac{1}{2}(\omega + ak^2 + k\alpha)\phi^2 + \frac{1}{4}(b_2 - k\lambda)\phi^4 + \frac{1}{6}b_3\phi^6 = h.$$

In this paper, we do not discuss the solutions of equation (7).

Generally, system (6) has the first integrals

$$H(\phi, y) = y^2(\phi^2 - a_0)^{\frac{1}{\beta}} + \frac{2}{\beta}\int\left[(\alpha_4\phi^8 + \alpha_2\phi^6 + \alpha_0\phi^4 + g_0)\phi^{-3}(\phi^2 - a_0)^{\frac{1}{\beta}-1}\right]d\phi = h. \tag{8}$$

When $\beta = 1$, i.e., $3\theta_1 = \theta_2 + \theta_3$, (8) becomes

$$H_1(\phi, y) = y^2(\phi^2 - a_0) + \frac{1}{3}\alpha_4\phi^6 + \frac{1}{2}\alpha_2\phi^4 + \alpha_0\phi^2 - \frac{g_0}{\phi^2} = h. \tag{9}$$

When $\beta = -1$, we see from (8) that

$$\begin{aligned} H_{-1}(\phi, y) = \tfrac{y^2}{\phi^2 - a_0} - \Big[&\alpha_4\phi^2 - \tfrac{g_0}{a_0\phi^2} + \tfrac{4g_0}{a_0^3}\ln(\phi) \\ &+ \Big(2a_0\alpha_4 + \alpha_2 - \tfrac{2g_0}{a_0^3}\Big)\ln(\phi^2 - a_0) - \tfrac{a_0^4\alpha_4 + a_0^3\alpha_2 + a_0^2\alpha_0 + g_0}{a_0^2(\phi^2 - a_0)}\Big] = h \end{aligned} \tag{10}$$

When $\beta = \frac{1}{2}$, we see from (8) that

$$\begin{aligned} H_{\frac{1}{2}}(\phi, y) = y^2(\phi^2 - a_0)^2 - \big[&-\tfrac{1}{2}\alpha_4\phi^8 + \tfrac{2}{3}(a_0\alpha_4 - \alpha_2)\phi^6 + (a_0\alpha_2 - \alpha_0)\phi^4 \\ &+ 2a_0\alpha_0\phi^2 - 4g_0\ln(\phi) - \tfrac{2a_0g_0}{\phi^2}\big] = h \end{aligned} \tag{11}$$

When $\beta = -\frac{1}{2}$, we see from (8) that

$$\begin{aligned} H_{-\frac{1}{2}}(\phi, y) = \tfrac{y^2}{(\phi^2 - a_0)^2} - \Big[&\tfrac{1}{a_0^4}\Big((6g_0 + 2a_0^4\alpha_4)\ln(\phi^2 - a_0) - 12g_0\ln(\phi) + \tfrac{2a_0g_0}{\phi^2}\Big) \\ &+ \tfrac{4g_0 - 4a_0^4\alpha_4 - 2a_0^3\alpha_2}{a_0^3(\phi^2 - a_0)} - \tfrac{g_0 + a_0^4\alpha_4 + a_0^3\alpha_2 + a_0^2\alpha_0}{a_0^2(\phi - a_0)^2}\Big] = h. \end{aligned} \tag{12}$$

Depending on different parameter β, the first integral $H_\beta(\phi, y) = h$ has various forms.

Obviously, for $a_0 > 0$, system (6) is a singular nonlinear traveling wave system of the first class defined in [14,15,16] with three singular straight lines $\phi = 0$ and $\phi = \pm\sqrt{a_0} = \mp\phi_s$. What is interesting is that singular traveling wave systems have peakon, periodic peakon, pseudo-peakon and compacton solution families. Corresponding to different types of phase orbits, in [14,15,16], the authors gave rise to a classification for different wave profiles of solution.

In this paper, we study the traveling wave solutions of system (6) via dynamical system approach. By presenting all possible bifurcations of phase portraits under different parameters conditions corresponding to system (6), we not only find all possible exact explicit parametric representations of solutions including solitary waves, periodic waves, kink and anti-kink wave, periodic peakons and peakons as well as compacton solutions, but also present very abounded dynamical behaviors.

The present paper is built up as follows. In section 2, we present bifurcations of phase portraits of system (6) when $\beta = 1$. In section 3 and section 4, we derive the exact expressions of solutions of system (6) under different parameter conditions. Finally, we demonstrate our conclusion in Section 5.

2 Bifurcations of phase portraits

In this section, we present bifurcations of phase portraits of system (6) depending on the parameter group $(a_0, \beta, g_0, \alpha_0, \alpha_2, \alpha_4)$. The corresponding regular system of system (6) is as follows

$$\frac{d\phi}{d\zeta} = \beta\phi^3(a_0 - \phi^2)y, \quad \frac{dy}{d\zeta} = \phi^4(y^2 + \alpha_0 + \alpha_2\phi^2 + \alpha_4\phi^4) + g_0, \tag{13}$$

where $d\xi = \beta\phi^3(a_0 - \phi^2)d\zeta$, for $\phi(a_0 - \phi^2) \neq 0$. System (13) has the same first integral as (8). But when $a_0 > 0$, the vector fields defined by system (13) and system (6) are different (see [16] and [18]).

We assume that $\alpha_0\alpha_2\alpha_4 \neq 0$. To discuss the equilibrium points $E_j(\phi_j, 0)$ of system (13), write that $F(\phi) = F_0(\phi) + g_0$, where $F_0(\phi) = \phi^4 f(\phi), f(\phi) = \alpha_0 + \alpha_2\phi^2 + \alpha_4\phi^4$. $F_0'(\phi) = 2\phi^3(2\alpha_0 + 3\alpha_2\phi^2 + 4\alpha_4\phi^4)$.

Clearly, we know the following fact.

(i) When $\Delta = \alpha_2^2 - 4\alpha_0\alpha_4 > 0, \Delta_1 = 9\alpha_2^2 - 32\alpha_0\alpha_4 > 0$ and $\alpha_0\alpha_4 > 0, \alpha_2\alpha_4 < 0, f(\phi)$ has two positive zeros $\phi_{1,2}$, $F_0'(\phi)$ has two positive zeros $\hat{\phi}_{1,2}$, where $\phi_1 < \phi_2$ and $\hat{\phi}_1 < \hat{\phi}_2$. When $\alpha_2 < 0, \alpha_4 > 0, \phi_1^2 = \frac{1}{2\alpha_4}(-\alpha_2 - \sqrt{\Delta}), \phi_2^2 = \frac{1}{2\alpha_4}(-\alpha_2 + \sqrt{\Delta}), \hat{\phi}_1 = \frac{1}{8\alpha_4}(-3\alpha_2 - \sqrt{\Delta_1}), \hat{\phi}_2 = \frac{1}{8\alpha_4}(-3\alpha_2 + \sqrt{\Delta_1})$; When $\alpha_2 > 0, \alpha_4 < 0, \phi_2^2 = \frac{1}{2\alpha_4}(-\alpha_2 - \sqrt{\Delta}), \phi_1^2 = \frac{1}{2\alpha_4}(-\alpha_2 + \sqrt{\Delta}), \hat{\phi}_1 = \frac{1}{8\alpha_4}(-3\alpha_2 + \sqrt{\Delta_1}), \hat{\phi}_2 = \frac{1}{8\alpha_4}(-3\alpha_2 - \sqrt{\Delta_1})$.

(ii) When $\Delta > 0, \alpha_0\alpha_4 < 0, f(\phi)$ has only one positive zero ϕ_e and $F_0'(\phi)$ has only one positive zero $\hat{\phi}_e$, where when $\alpha_4 > 0, \phi_e^2 = \frac{1}{2\alpha_4}(-\alpha_2 + \sqrt{\Delta}), \hat{\phi}_e = \frac{1}{8\alpha_4}(-3\alpha_2 + \sqrt{\Delta_1})$; when $\alpha_4 < 0, \phi_e^2 = \frac{1}{2\alpha_4}(-\alpha_2 - \sqrt{\Delta}), \hat{\phi}_e = \frac{1}{8\alpha_4}(-3\alpha_2 - \sqrt{\Delta_1})$.

(iii) When $\Delta = 0$ and $\alpha_2\alpha_4 < 0, f(\phi)$ has a positive double zero $\phi_d = \sqrt{-\frac{\alpha_2}{2\alpha_4}}$.

Let

$$g^* = F_0(\hat{\phi}_1) = \hat{\phi}_1^4 f(\hat{\phi}_1), \quad g_e^* = F_0(\hat{\phi}_e) = \hat{\phi}_e^4 f(\hat{\phi}_e). \tag{14}$$

Then, it is easy to see that the following conclusions hold.

(1) When $\Delta = \alpha_2^2 - 4\alpha_0\alpha_4 > 0$ and $\alpha_0\alpha_4 > 0, \alpha_2 < 0, \alpha_4 > 0, -g^* < g_0 < 0$, (or $\alpha_0\alpha_4 > 0, \alpha_2 > 0, \alpha_4 < 0, 0 < g_0 < |g^*|$), then, equation (6) has six equilibrium points $E_{j\mp}(\mp\phi_j, 0), j = 1, 2, 3$ satisfying $0 < \phi_1 < \hat{\phi}_1 < \phi_2 < \hat{\phi}_2 < \phi_3$.

(2) When $\Delta > 0, \alpha_0 < 0, \alpha_4 > 0, 0 < g_0 < |g_e^*|$ (or $\alpha_0 > 0, \alpha_4 < 0, -g_e^* < g_0 < 0$), then, equation (6) has four equilibrium points $E_{j\mp}(\mp\phi_j, 0), j = 1, 2$ satisfying $0 < \phi_1 < \hat{\phi}_e < \phi_2$.

In addition, when $a_0 > 0$, if $Y_s = \frac{1}{a_0^2}[g_0 - a_0^2(\alpha_0 + \alpha_2 a_0 + \alpha_4 a_0^2)] > 0$, then, there are four equilibrium points at $E_{sj}(\mp\sqrt{a_0}, \mp\sqrt{Y_s}), j = 1, 2, 3, 4$ of system (9) in two straight lines $\phi = \mp\sqrt{a_0}$.

Taking $M(\phi_j, y_j)$ be the coefficient matrix of the linearized system of system (9) at equilibrium point $E_j(\phi_j, y_j)$ and $J(\phi_j, y_j) = \mathrm{detM}(\phi_j, y_j)$. We have

$$J(\phi_j, 0) = -\beta(a_0 - \phi_j^2)\phi_j^3 F_0'(\phi_j), \quad J(\sqrt{a_0}, \sqrt{Y_s}) = -4\beta a_0^4 Y_s.$$

By the theory of planar dynamical systems, for an equilibrium point of a planar integrable system, if $J < 0$, then the equilibrium point is a saddle point; If $J > 0$ and $(\mathrm{Trace}M)^2 - 4J < 0 (> 0)$, then the equilibrium point is a center point (a node point); if $J = 0$ and the Poincaré index of the equilibrium point is 0, then it is a cusp.

Write that $h_j = H_1(\phi_j, 0)$ and $h_s = H_1(\sqrt{a_0}, \sqrt{Y_s}) = 0$, where $H_1(\phi, y) = h$ is defined by (8).

First, we assume that $\Delta > 0, \alpha_0 < 0, \alpha_4 > 0, 0 < g_0 < |g_e^*|$. Now, system (6) has four symmetric equilibrium points. Based on the above information to make qualitative analysis, for $\beta = 1$ and a fixed parameter group $(\alpha_0, \alpha_2, \alpha_4, g_0)$, as a_0 is varied, we obtain the bifurcations of the phase portraits of system (6) shown in Fig.1 (a)-(g).

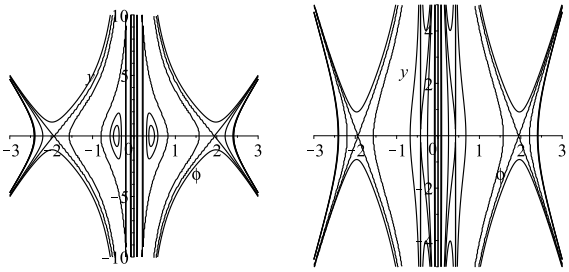

(a) $0 < a_0 < \phi_1$ (b) $a_0 = \phi_1$

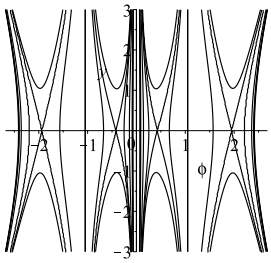

(c) $\phi_1 < a_0 < \phi_2$

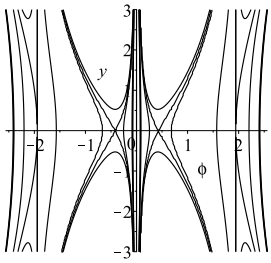

(d) $a_0 = \phi_2$

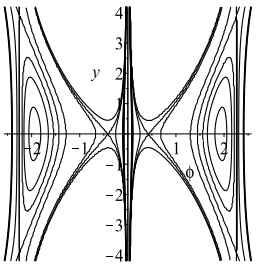

(e) $\phi_2 < a_0, h_s > h_1$

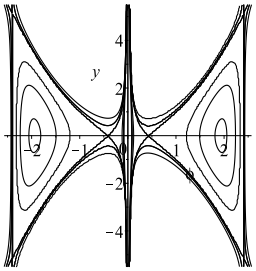

(f) $\phi_2 < a_0, h_s = h_1$

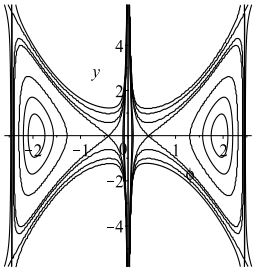

(g) $\phi_2 < a_0, h_s < h_1$

Fig.1 The bifurcations of phase portraits of system (6) when $F(\phi)$ has four zeros

Second, we assume that $\Delta = \alpha_2^2 - 4\alpha_0\alpha_4 > 0$ and $\alpha_0\alpha_4 > 0, \alpha_2 < 0, \alpha_4 > 0, -g^* < g_0 < 0$. In this case, system (6) has six symmetric equilibrium points. For $\beta = 1$ and a fixed parameter group $(\alpha_0, \alpha_2, \alpha_4, g_0)$, as a_0 is varied, we have the bifurcations of the phase portraits of system (6) presented in Fig.2 (a)-(m).

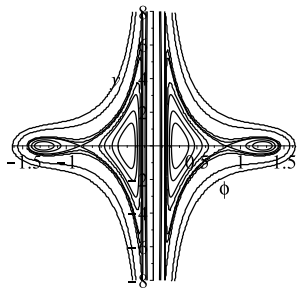

(a) $0 < a_0 < \phi_1, h_2 < h_s$

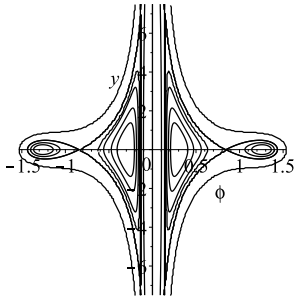

(b) $0 < a_0 < \phi_1, h_2 = h_s$

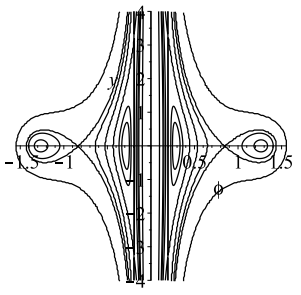

(c) $0 < a_0 < \phi_1, h_2 > h_s$

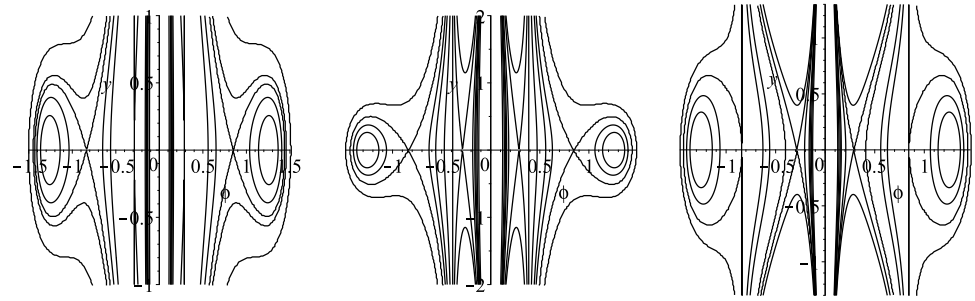

(d) $a_0 = \phi_1$ (e) $\phi_1 < a_0 < \phi_2$ (f) $a_0 = \phi_2$

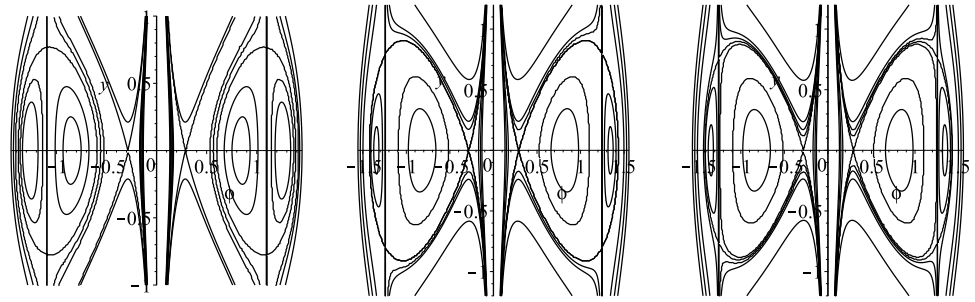

(g) $\phi_2 < a_0 < \phi_3, h_1 < h_s$ (h) $\phi_2 < a_0 < \phi_3, h_1 = h_s$ (i) $\phi_2 < a_0 < \phi_3, h_1 > h_s$

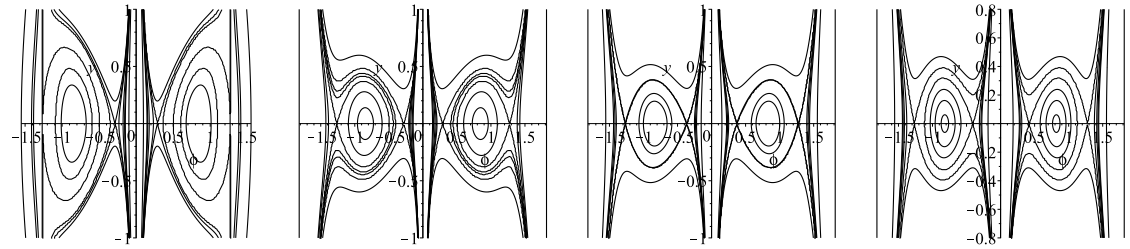

(j) $a_0 = \phi_3$ (k) $a_0 > \phi_3, h_1 < h_3$ (l) $a_0 > \phi_3, h_1 = h_3$ (m) $a_0 > \phi_3, h_1 > h_3$

Fig.2 The bifurcations of phase portraits of system (6) when $F(\phi)$ has six zeros

3 Exact solutions of system (6) when there exist four equilibrium points in Fig.1

In this section, under the parameter conditions $\Delta = \alpha_2^2 - 4\alpha_0\alpha_4 > 0, \alpha_0 < 0, \alpha_4 > 0, 0 < g_0 < |g_e^*|$, we discuss possible parametric representations of the level curves defined by $H_1(\phi, y) = h$ in (9).

Notice that $H_1(\phi, y) = h$ can be written as

$$y^2 = \frac{g_0 + h\phi^2 - \alpha_0\phi^4 - \frac{1}{2}\alpha_2\phi^6 - \frac{1}{3}\alpha_4\phi^8}{\phi^2(\phi^2 - a_0)} \equiv \frac{\frac{\alpha_4}{3}F_8(\phi)}{\phi^2(\phi^2 - a_0)}. \tag{15}$$

Assume that $\alpha_4 > 0$, then, using the first equation of system (6), we know that

$$\sqrt{\frac{\alpha_4}{3}}\xi = \int_{\phi_0}^{\phi} \sqrt{\frac{\phi^2(\phi^2 - a_0)}{F_8(\phi)}}d\phi = \int_{\psi_0}^{\psi} \frac{|\psi - a_0|d\psi}{2\sqrt{|\psi - a_0|F_4(\psi)}}, \tag{16}$$

where $\psi = \phi^2, F_4(\psi) = \frac{3g_0}{\alpha_4} + \frac{3h}{\alpha_4}\psi - \frac{3\alpha_0}{\alpha_4}\psi^2 - \frac{3\alpha_2}{2\alpha_4}\psi^3 - \psi^4$. Obviously, if and only if polynomial $F_4(\psi)$ can be decomposed into a product of a double linear factor and a quadratic factor, then the integral (16) can be solved.

(i) Corresponding to the two arch orbits defined by $H_1(\phi, y) = h_s$ in Fig.1 (a), we have $F_4(\psi) = (\psi_a - \psi)(\psi_M - \psi)(\psi - a_0)(\psi + \psi_i)$. Thus, (16) becomes $2\sqrt{\frac{\alpha_4}{3}}\xi = \int_{\psi}^{\psi_M} \frac{d\psi}{\sqrt{(\psi_a-\psi)(\psi_M-\psi)(\psi+\psi_i)}}$. System (6) has the periodic peakon solutions of the following form

$$\phi(\xi) = \mp\left(\psi_a - \frac{\psi_a - \psi_M}{\mathrm{dn}^2(\Omega_1\xi, k)}\right)^{\frac{1}{2}}, \quad \xi \in (-\xi_{01}, \xi_{01}), \tag{17}$$

where $\Omega_1 = \sqrt{\frac{\alpha_4(\psi_a+\psi_i)}{3}}, k^2 = \frac{\psi_M+\psi_i}{\psi_a+\psi_i}, \xi_{01} = \frac{1}{\Omega_1}\mathrm{dn}^{-1}\sqrt{\frac{\psi_a-\psi_M}{\psi_a-a_0}}$.

(ii) The level curves defined by $H_1(\phi, y) = h_s$ in Fig.1 (e) contain two arches and two open curves which tend to the singular straight line $\phi = 0$ when $|y| \to \infty$. For the arches, integral (16) becomes $2\sqrt{\frac{\alpha_4}{3}}\xi = \int_{\psi_m}^{\psi} \frac{d\psi}{\sqrt{(\psi-\psi_m)(\psi-\psi_l)(\psi+\psi_i)}}$. For the right open curve, (16) has the form $2\sqrt{\frac{\alpha_4}{3}}\xi = \int_{\psi}^{\psi_l} \frac{d\psi}{\sqrt{(\psi_m-\psi)(\psi_l-\psi)(\psi+\psi_i)}}$. Hence, we obtain two periodic peakon solutions (see Fig.3 (a)) and two compacton solutions (see Fig.3 (b)) as follows

$$\phi(\xi) = \mp\left(\psi_l + \frac{\psi_m - \psi_l}{\mathrm{cn}^2(\Omega_2\xi, k)}\right)^{\frac{1}{2}}, \quad \xi \in (-\xi_{02}, \xi_{02}) \tag{18}$$

where $\Omega_2 = \sqrt{\frac{\alpha_4(\psi_m+\psi_i)}{3}}, k^2 = \frac{\psi_l+\psi_i}{\psi_m+\psi_i}, \xi_{02} = \frac{1}{\Omega_2}\mathrm{cn}^{-1}\sqrt{\frac{\psi_m-\psi_l}{a_0-\psi_l}}$; And

$$\phi(\xi) = \mp\left(\psi_m - \frac{\psi_m - \psi_l}{\mathrm{dn}^2(\Omega_3\xi, k)}\right)^{\frac{1}{2}}, \quad \xi \in (-\xi_{03}, \xi_{03}), \tag{19}$$

where $\Omega_3 = \sqrt{\frac{\alpha_4(\psi_m+\psi_i)}{3}}, k^2 = \frac{\psi_l+\psi_i}{\psi_m+\psi_i}, \xi_{03} = \frac{1}{\Omega_3}\mathrm{dn}^{-1}\sqrt{1 - \frac{\psi_l}{\psi_m}}$.

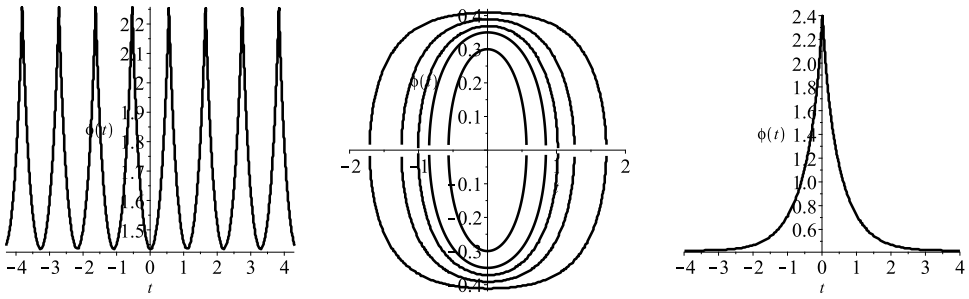

(a) Periodic peakon (b) Compactons (c) Peakon

Fig.3 The profiles of periodic peakon, compactons and peakon of system (6)

(iii) The level curves defined by $H_1(\phi, y) = h_s$ in Fig.1 (f) are two curve triangles. Now, (16) becomes that $2\sqrt{\frac{\alpha_4}{3}}\xi = \int_{\psi}^{a_0} \frac{d\psi}{(\psi-\psi_1)\sqrt{\psi+\psi_i}}$. It gives rise the following peakon (see Fig.3 (c)) and anti-peakon solutions

$$\phi(\xi) = \mp\left(-\psi_i + (\psi_1+\psi_i)\mathrm{ctnh}^2(\omega_1|\xi| + \xi_{04})\right)^{\frac{1}{2}}, \tag{20}$$

where $\omega_1 = \sqrt{\frac{\alpha_4(\psi_1+\psi_i)}{3}}, \xi_{04} = \mathrm{ctnh}^{-1}\sqrt{\frac{a_0+\psi_i}{\psi_1+\psi_i}}$.

(iv) The level curves defined by $H_1(\phi, y) = h_1$ in Fig.1 (g) are two homoclinic orbits to the equilibrium points $E_1(\phi_1, 0)$ and its symmetric point with respect to $y-$axis. In this case, (16) can be written as

$$2\sqrt{\frac{\alpha_4}{3}}\xi = \int_{\psi}^{\psi_M} \frac{(a_0-\psi)d\psi}{(\psi-\psi_1)\sqrt{(a_0-\psi)(\psi_M-\psi)(\psi+\psi_i)}}.$$

It gives rise to the following solitary wave solutions

$$\begin{aligned} \phi(\chi) &= \mp\left(a_0 - \frac{a_0-\psi_M}{\mathrm{dn}^2(\chi,k)}\right)^{\frac{1}{2}}, \quad \chi \in (-\chi_{01}, \chi_{01}), \\ \xi(\chi) &= \sqrt{\frac{3}{\alpha_4(a_0+\psi_i)}}\left[2\chi \pm \frac{a_0-\psi_M}{\psi_M-\psi_1}\Pi(\arcsin(\mathrm{sn}(\chi,k)), \hat{\alpha}_1^2, k)\right], \end{aligned} \tag{21}$$

where $k^2 = \frac{\psi_M+\psi_i}{a_0+\psi_i}, \hat{\alpha}_1^2 = \frac{k^2(a_0-\psi_1)}{\psi_M-\psi_1}, \chi_{01} = \mathrm{dn}^{-1}\sqrt{\frac{a_0-\psi_M}{a_0-\psi_1}}$ and $\Pi(\cdot,\cdot,k)$ is the elliptic integral of the third kind.

4 Exact solutions of system (6) when there exist six equilibrium points in Fig.2

In this section, under the parameter conditions $\Delta = \alpha_2^2 - 4\alpha_0\alpha_4 > 0$ and $\alpha_0\alpha_4 > 0, \alpha_2 < 0, \alpha_4 > 0, -g^* < g_0 < 0$, we discuss possible parametric representations of the level curves defined by $H_1(\phi, y) = h$ in (9).

(1) Consider the phase portrait in Fig.2 (a). When h is varied, the changes of the level curves defined by$H_1(\phi, y) = h$ are shown in Fig.4.

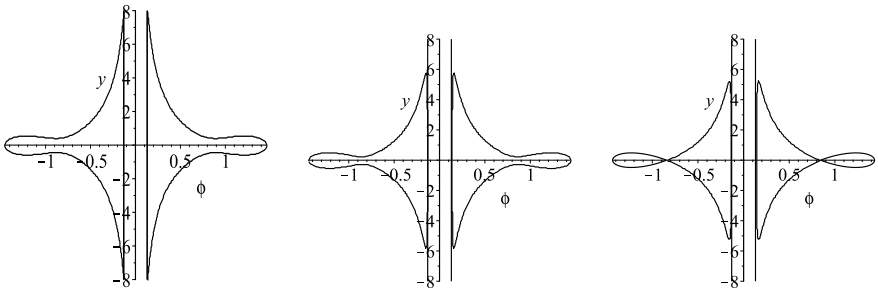

(a) $h = h_s$ (b) $h \in (h_s, h_2)$ (c) $h = h_2$

Fig.4 The level curves defined by $H_1(\phi, y) = h$ of system (6) in Fig.2 (a)

(i) The level curves defined by $H_1(\phi, y) = h_s$ are two arch orbits enclosing three equilibrium points $E_{\mp j}(\mp\phi_j, 0), j = 1, 2, 3$, respectively. In this case, (16) can be written as $2\sqrt{\frac{\alpha_4}{3}}\xi = \int_{\psi}^{\psi_M} \frac{d\psi}{\sqrt{(\psi_M-\psi)[(\psi-\hat{b}_1)^2+\hat{a}_1^2]}}$. It gives rise to the following two periodic peakon solutions

$$\phi(\xi) = \mp\left(\frac{\psi_M - A_1 + (A_1+\psi_M)\mathrm{cn}(\Omega_4\xi, k)}{1+\mathrm{cn}(\Omega_4\xi, k)}\right)^{\frac{1}{2}}, \quad \xi \in (-\xi_{05}, \xi_{05}) \tag{22}$$

where $\Omega_4 = \sqrt{\frac{\alpha_4 A_1}{3}}, k^2 = \frac{A_1+\psi_M-\hat{b}_1}{2A_1}, \xi_{05} = \frac{1}{\Omega_4}\mathrm{cn}^{-1}\left(\frac{A_1-\psi_M+a_0}{A_1+\psi_M-a_0}\right)$.

(ii) The level curves defined by $H_1(\phi, y) = h_2$ are four homoclinic orbits with "eight figure" to the two equilibrium points $E_{\mp 2}(\mp\phi_2, 0)$, respectively. In this case, (16) can be written as $2\sqrt{\frac{\alpha_4}{3}}\xi = \int_{\psi}^{\psi_M} \frac{(\psi-a_0)d\psi}{(\psi-\psi_2)\sqrt{(\psi_M-\psi)(\psi-\psi_m)(\psi-a_0)}}$ and $2\sqrt{\frac{\alpha_4}{3}}\xi = \int_{\psi_m}^{\psi} \frac{(\psi-a_0)d\psi}{(\psi_2-\psi)\sqrt{(\psi_M-\psi)(\psi-\psi_m)(\psi-a_0)}}$. Thus, we obtain the following two solitary wave solutions and two pseudo-peakon solutions

$$\begin{aligned} \phi(\chi) &= \mp\left(\psi_M - (\psi_M-\psi_m)\mathrm{sn}^2(\chi, k)\right)^{\frac{1}{2}}, \quad \chi \in (-\chi_{02}, \chi_{02}), \\ \xi(\chi) &= \sqrt{\frac{3}{\alpha_4(\psi_M-a_0)}}\left[\chi \pm \left(\frac{\psi_2-a_0}{\psi_M-\psi_2}\right)\Pi(\arcsin(\mathrm{sn}(\chi, k)), \hat{\alpha}_2^2, k)\right], \end{aligned} \tag{23}$$

where $k^2 = \frac{\psi_M-\psi_m}{\psi_M-a_0}, \hat{\alpha}_2^2 = \frac{\psi_M-\psi_m}{\psi_M-\psi_2}, \chi_{02} = \mathrm{sn}^{-1}\sqrt{\frac{\psi_M-\psi_2}{\psi_M-\psi_m}}$; and

$$\begin{aligned} \phi(\chi) &= \mp\left(a_0 + \frac{\psi_M-a_0}{\mathrm{dn}^2(\chi, k)}\right)^{\frac{1}{2}}, \quad \chi \in (-\chi_{03}, \chi_{03}), \\ \xi(\chi) &= \pm\sqrt{\frac{3}{\alpha_4(\psi_M-a_0)}}\left(\frac{\psi_m-a_0}{\psi_2-a_0}\right)\Pi(\arcsin(\mathrm{sn}(\chi, k)), \hat{\alpha}_3^2, k), \end{aligned} \tag{24}$$

where $k^2 = \frac{\psi_M-\psi_m}{\psi_M-a_0}, \hat{\alpha}_3^2 = \frac{k^2(\psi_2-a_0)}{\psi_2-\psi_m}, \chi_{03} = \mathrm{dn}^{-1}\sqrt{\frac{\psi_m-a_0}{\psi_2-a_0}}$.

(2) Consider the phase portrait in Fig.2 (b). The level curves defined by $H_1(\phi, y) = h_s$ contain two homoclinic orbits to the two equilibrium points

$E_{\mp 2}(\mp\phi_2, 0)$, respectively, and two curve triangles enclosing the two equilibrium points $E_{\mp 2}(\mp\phi_1, 0)$, respectively. In this case, (16) can be written as $2\sqrt{\frac{\alpha_4}{3}}\xi = \int_{\psi}^{\psi_M} \frac{d\psi}{(\psi-\psi_2)\sqrt{(\psi_M-\psi)}}$ and $2\sqrt{\frac{\alpha_4}{3}}\xi = \int_{a_0}^{\psi} \frac{d\psi}{(\psi_2-\psi)\sqrt{(\psi_M-\psi)}}$. Hence, system (6) have two solitary wave solutions, a peakon and an anti-peakon solution as follows (see Fig.5)

$$\phi(\xi) = \mp\left(\psi_M - (\psi_M - \psi_2)\tanh^2(\omega_2\xi)\right)^{\frac{1}{2}}, \tag{25}$$

where $\omega_2 = \sqrt{\frac{\alpha_4(\psi_M-\psi_2)}{3}}$; and

$$\phi(\xi) = \mp\left(\psi_M - (\psi_M - \psi_2)\mathrm{ctnh}^2(\omega_2|\xi| + \xi_{05})\right)^{\frac{1}{2}}, \tag{26}$$

where $\xi_{05} = \mathrm{ctnh}^{-1}\sqrt{\frac{\psi_M-a_0}{\psi_M-\psi_2}}$.

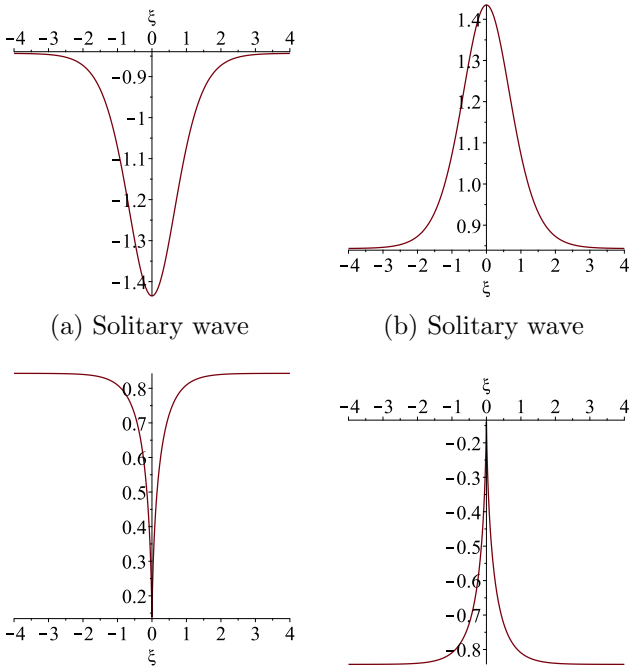

(a) Solitary wave (b) Solitary wave

(c) Anti-peakon (d) Peakon

Fig.5 The profiles of solitary waves and peakon, anti-peakon of system (6) given by (25), (26)

(3) Consider the phase portrait in Fig.2 (c).

(i) The level curves defined by $H_1(\phi, y) = h_s$ are two arch orbits enclosing the equilibrium points $E_{\mp 1}(\mp\phi_1, 0)$, respectively. They has the same parametric representations as (22) and give rise to two periodic peakon solutions.

(ii) The level curves defined by $H_1(\phi,y)=h_3$ in Fig.2 (c) contain two homoclinic orbits to the equilibrium points $E_2(\phi_2,0)$ and its symmetric point with respect to $y-$axis and two open curves which tend to the singular straight line $\phi=0$ when $|y|\to\infty$. In this case, (16) can be written as $2\sqrt{\frac{\alpha_4}{3}}\xi=\int_{\psi}^{\psi_M}\frac{(\psi-a_0)d\psi}{(\psi-\psi_2)\sqrt{(\psi_M-\psi)(\psi-a_0)(\psi-\psi_l)}}$ and $2\sqrt{\frac{\alpha_4}{3}}\xi=\int_{\psi}^{\psi_l}\frac{(a_0-\psi)d\psi}{(\psi_2-\psi)\sqrt{(\psi_M-\psi)(a_0-\psi)(\psi_l-\psi)}}$.
Two homoclinic orbits give rise to the following two solitary wave solutions

$$\begin{aligned}&\phi(\chi)=\mp\left(\psi_M-(\psi_M-a_0)\mathrm{sn}^2(\chi,k)\right)^{\frac{1}{2}},\quad \chi\in(-\chi_{04},\chi_{04}),\\ &\xi(\chi)=\sqrt{\frac{3}{\alpha_4(\psi_M-\psi_l)}}\left[\chi\pm\left(\frac{\psi_2-a_0}{\psi_M-\psi_2}\right)\Pi(\arcsin(\mathrm{sn}(\chi,k)),\hat{\alpha}_4^2,k)\right],\end{aligned}\tag{27}$$

where $k^2=\frac{\psi_M-a_0}{\psi_M-\psi_l},\hat{\alpha}_4^2=\frac{\psi_M-a_0}{\psi_M-\psi_l},\chi_{04}=\mathrm{sn}^{-1}\sqrt{\frac{\psi_M-\psi_2}{\psi_M-a_0}}$.
Two open orbits give rise to the following two compacton solutions

$$\begin{aligned}&\phi(\chi)=\mp\left(a_0-\frac{a_0-\psi_l}{\mathrm{cn}^2(\chi,k)}\right)^{\frac{1}{2}},\quad \chi\in(-\chi_{05},\chi_{05}),\\ &\xi(\chi)=\pm\sqrt{\frac{3}{\alpha_4(\psi_M-\psi_l)}}\left[\left(\frac{a_0-\psi_l}{\psi_2-\psi_l}\right)\Pi(\arcsin(\mathrm{sn}(\chi,k)),\hat{\alpha}_5^2,k)\right],\end{aligned}\tag{28}$$

where $k^2=\frac{\psi_M-a_0}{\psi_M-\psi_l},\hat{\alpha}_5^2=\frac{\psi_2-a_0}{\psi_2-\psi_l},\chi_{05}=\mathrm{cn}^{-1}\sqrt{1-\frac{\psi_l}{a_0}}$.

(4) Consider the phase portraits in Fig.2 (d) and (e). The level curves defined by $H_1(\phi,y)=h_3$ in these phase portraits contain two homoclinic orbits to the equilibrium points $E_2(\phi_2,0)$ and its symmetric point with respect to $y-$axis and two open curves which tend to the singular straight line $\phi=0$ when $|y|\to\infty$. They have the same parametric representations as (27) and (28).

(5) Consider the phase portrait in Fig.2 (f). The level curves defined by $H_1(\phi,y)=h_s$ are two oval orbits enclosing the equilibrium points $E_{\mp1}(\mp\phi_3,0)$, respectively, and two open curves which tend to the singular straight line $\phi=0$ when $|y|\to\infty$. Now, (16) becomes that $2\sqrt{\frac{\alpha_4}{3}}\xi=\int_{\psi}^{\psi_M}\frac{d\psi}{\sqrt{(\psi_M-\psi)(\psi-a_0)(\psi-\psi_l)}}$ and $2\sqrt{\frac{\alpha_4}{3}}\xi=\int_{\psi}^{\psi_l}\frac{d\psi}{\sqrt{(\psi_M-\psi)(a_0-\psi)(\psi_l-\psi)}}$. Thus, the two oval orbits give rise to two periodic solutions as follows

$$\phi(\xi)=\mp\left(\psi_M-(\psi_M-a_0)\mathrm{sn}^2(\Omega_5\xi,k)\right)^{\frac{1}{2}},\tag{29}$$

where $k^2=\frac{\psi_M-a_0}{\psi_M-\psi_l},\Omega_5=\sqrt{\frac{\alpha_4(\psi_M-\psi_l)}{3}}$. The two open orbits give rise to two compacton solutions as follows

$$\phi(\xi)=\mp\left(a_0-\frac{a_0-\psi_l}{\mathrm{cn}(\Omega_5\xi,k)}\right)^{\frac{1}{2}},\quad \xi\in(-\xi_{06},\xi_{06}),\tag{30}$$

where $k^2=\frac{\psi_M-a_0}{\psi_M-\psi_l},\xi_{06}=\frac{1}{\Omega_5}\mathrm{cn}^{-1}\sqrt{1-\frac{\psi_l}{a_0}}$.

(6) Consider the phase portrait in Fig.2 (g). The level curves defined by $H_1(\phi, y) = h_s$ contain two oval orbits which are transverse to the singular straight line $\phi = \mp\sqrt{a_0}$ and enclose the two equilibrium points $E_{\mp j}(\mp\phi_j, 0), j = 2, 3$, respectively, and two open curves which tend to the singular straight line $\phi = 0$ when $|y| \to \infty$. Now, (16) becomes that $2\sqrt{\frac{\alpha_4}{3}}\xi = \int_{\psi}^{\psi_M} \frac{d\psi}{\sqrt{(\psi_M-\psi)(\psi-\psi_m)(\psi-\psi_l)}}$ and $2\sqrt{\frac{\alpha_4}{3}}\xi = \int_{\psi}^{\psi_l} \frac{d\psi}{\sqrt{(\psi_M-\psi)(\psi_m-\psi)(\psi_l-\psi)}}$.

Two oval curves give rise to the following periodic solutions

$$\phi(\xi) = \mp\left(\psi_M - (\psi_M - \psi_m)\mathrm{sn}(\Omega_6\xi, k)\right)^{\frac{1}{2}}, \tag{31}$$

where $k^2 = \frac{\psi_M-\psi_m}{\psi_M-\psi_l}, \Omega_6 = \sqrt{\frac{\alpha_4(\psi_m-\psi_l)}{3}}$.

As a limit orbit of the family of closed orbits enclosing the equilibrium points $E_3(\phi_3, 0)$, the arch in the right of the singular straight line $\phi = \sqrt{a_0}$ has the parametric representation

$$\phi(\xi) = \left(\psi_M - (\psi_M - \psi_m)\mathrm{sn}(\Omega_6\xi, k)\right)^{\frac{1}{2}}, \quad \xi \in (-\xi_{07}, \xi_{07}), \tag{32}$$

where $\xi_{07} = \frac{1}{\Omega_6}\mathrm{sn}^{-1}\sqrt{\frac{\psi_M-a_0}{\psi_M-\psi_m}}$.

As a limit orbit of the family of closed orbits enclosing the equilibrium points $E_2(\phi_2, 0)$, the arch in the left of the singular straight line $\phi = \sqrt{a_0}$ has the parametric representation

$$\phi(\xi) = \left(\psi_M - (\psi_M - \psi_m)\mathrm{sn}(\Omega_6\xi, k)\right)^{\frac{1}{2}}, \quad \xi \in \left(\frac{2K(k)}{\Omega_6} - \xi_{07}, \frac{2K(k)}{\Omega_6} + \xi_{07}\right), \tag{33}$$

where $K(k)$ is the complete elliptic integral of the first kind. (32) and (33) define two periodic peakons.

The two open orbits give rise to two compacton solutions as follows

$$\phi(\xi) = \mp\left(\psi_M - \frac{\psi_m - \psi_l}{\mathrm{cn}^2(\Omega_8\xi, k)}\right)^{\frac{1}{2}}, \quad \xi \in (-\xi_{08}, \xi_{08}), \tag{34}$$

where $k^2 = \frac{\psi_M-\psi_m}{\psi_M-\psi_l}, \Omega_8 = \sqrt{\frac{\alpha_4(\psi_M-\psi_m)}{3}}, \xi_{08} = \frac{1}{\Omega_8}\mathrm{cn}^{-1}\sqrt{1-\frac{\psi_l}{\psi_m}}$.

(7) Consider the phase portrait in Fig.2 (h). The level curves defined by $H_1(\phi, y) = h_s$ contain two homoclinic orbits to the equilibrium points $E_{1\mp}(\mp\phi_1, 0)$, which are transverse to the singular straight line $\phi = \mp\sqrt{a_0}$ and enclose the two equilibrium points $E_{j\mp}(\mp\phi_j, 0), j = 2, 3$, respectively. Now, (16) can be written as $2\sqrt{\frac{\alpha_4}{3}}\xi = \int_{\psi}^{\psi_M} \frac{d\psi}{(\psi-\psi_1)\sqrt{(\psi_M-\psi)}}$. It gives rise to the following two solitary wave solutions (see Fig.6 (a))

$$\phi(\xi) = \mp\left(\psi_M - (\psi_M - \psi_1)\tanh^2(\omega_3\xi)\right)^{\frac{1}{2}}, \tag{35}$$

where $\omega_3 = \sqrt{\frac{\alpha_4(\psi_M-\psi_1)}{3}}$.

The two curve triangles enclosing the equilibrium points $E_{2\mp}(\mp\phi_1,0)$ have the parametric representations

$$\phi(\xi)=\mp\left(\psi_M-(\psi_M-\psi_1)\tanh^2(\omega_3|\xi|+\xi_{09})\right)^{\frac{1}{2}}, \tag{36}$$

where $\xi_{09}=\tanh^{-1}\sqrt{\frac{\psi_M-a_0}{\psi_M-\psi_1}}$. (36) define a peakon and an anti-peakon solutions (see Fig.6 (b)).

The two arches enclosing the equilibrium points $E_{3\mp}(\mp\phi_3,0)$ have the parametric representations

$$\phi(\xi)=\mp\left(\psi_M-(\psi_M-\psi_1)\tanh^2(\omega_3\xi)\right)^{\frac{1}{2}}, \quad \xi\in(-\xi_{09},\xi_{09}), \tag{37}$$

(37) gives rise to two periodic peakon solutions (see Fig.6 (d)).

(8) Consider the phase portrait in Fig.2 (i).

(i) The level curves defined by $H_1(\phi,y)=h_1$ contain two homoclinic orbits to the equilibrium points $E_{1\mp}(\mp\phi_1,0)$, respectively, and two open orbits which tend to two singular straight lines $\phi=\mp\sqrt{a_0}$, respectively, when $|y|\to\infty$. In this case, (16) can be written as $2\sqrt{\frac{\alpha_4}{3}}\xi=\int_{\psi}^{\psi_M}\frac{(a_0-\psi)d\psi}{(\psi-\psi_1)\sqrt{(\psi_L-\psi)(a_0-\psi)(\psi_M-\psi)}}$ and $2\sqrt{\frac{\alpha_4}{3}}\xi=\int_{\psi}^{\psi_L}\frac{(\psi-a_0)d\psi}{(\psi-\psi_1)\sqrt{(\psi_L-\psi)(\psi-a_0)(\psi-\psi_M)}}$.

The two homoclinic orbits give rise to two solitary wave solutions (or pseudo-peakon solutions) as follows (see Fig.6 (c))

$$\begin{aligned}&\phi(\xi)=\mp\left(a_0-\frac{a_0-\psi_M}{\mathrm{cn}^2(\chi,k)}\right)^{\frac{1}{2}}, \quad \chi\in(-\chi_{06},\chi_{06}),\\ &\xi(\chi)=\pm\sqrt{\frac{3}{\alpha_4(\psi_L-\psi_M)}}\left(\frac{a_0-\psi_M}{\psi_M-\psi_1}\right)\Pi(\arcsin(\mathrm{sn}(\chi,k),\hat{\alpha}_5^2,k),\end{aligned} \tag{38}$$

where $k^2=\frac{\psi_L-a_0}{\psi_L-\psi_M},\hat{\alpha}_5^2=\frac{a_0-\psi_1}{\psi_M-\psi_1},\chi_{06}=\mathrm{cn}^{-1}\sqrt{\frac{a_0-\psi_M}{a_0-\psi_1}}$. The two open orbits give rise to two compacton solutions as follows

$$\begin{aligned}&\phi(\xi)=\mp\left(\psi_L-(\psi_L-a_0)\mathrm{sn}^2(\chi,k)\right)^{\frac{1}{2}}, \quad \chi\in(-K(k),K(k)),\\ &\xi(\chi)=\pm\sqrt{\frac{3}{\alpha_4(\psi_L-\psi_M)}}\left[\chi-\left(\frac{a_0-\psi_1}{\psi_L-\psi_1}\right)\Pi(\arcsin(\mathrm{sn}(\chi,k),\hat{\alpha}_6^2,k)\right],\end{aligned} \tag{39}$$

where $k^2=\frac{\psi_L-a_0}{\psi_L-\psi_M},\hat{\alpha}_6^2=\frac{\psi_L-a_0}{\psi_L-\psi_1}$.

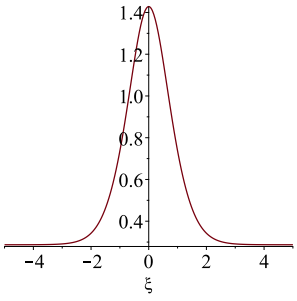

(a) Solitary wave

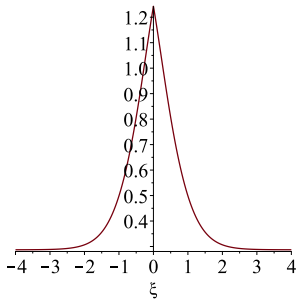

(b) Peakon

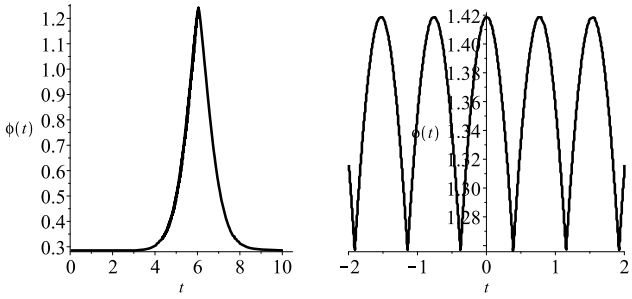

(c) Pseudo-peakon (d) Periodic peakon

Fig.6 The profiles of solitary wave, pseudo-peakon, peakon and periodic peakon of system (6)

(ii) The level curves defined by $H_1(\phi, y) = h_s$ contain two open curves passing through the singular straight lines $\phi = \mp\sqrt{a_0}$, respectively, and tending to the singular straight line $\phi = 0$. As the limit curves of the periodic orbit families enclosing the equilibrium points $E_{3\mp}(\mp\phi_3, 0)$, two arches give rise to two periodic peakon solutions. In fact, in this case, (16) can be written as $2\sqrt{\frac{\alpha_4}{3}}\xi = \int_{\psi}^{\psi_M} \frac{d\psi}{\sqrt{(\psi_M-\psi)[(\psi-b_2)^2+a_2^2]}}$. Thus, two periodic peakon solutions have the same parametric representations as (22). Two full open curves give rise to two compacton solutions given by

$$\phi(\xi) = \mp\left(\frac{\psi_M - A_1 + (A_1+\psi_M)\mathrm{cn}(\Omega_4\xi, k)}{1+\mathrm{cn}(\Omega_4\xi, k)}\right)^{\frac{1}{2}}, \quad \xi \in (-\xi_{10}, \xi_{10}) \tag{40}$$

where $\Omega_4 = \sqrt{\frac{\alpha_4 A_1}{3}}, k^2 = \frac{A_1+\psi_M-\hat{b}_1}{2A_1}, \xi_{10} = \frac{1}{\Omega_4}\mathrm{cn}^{-1}\left(\frac{A_1-\psi_M}{A_1+\psi_M}\right)$.

(9) Consider the phase portrait in Fig.2 (j).

The level curves defined by $H_1(\phi, y) = h_s$ are two oval orbits enclosing the equilibrium points $E_{\mp 2}(\mp\phi_2, 0)$, respectively, and two open curves which tend to the singular straight line $\phi = 0$ when $|y| \to \infty$. Now, (16) becomes that $2\sqrt{\frac{\alpha_4}{3}}\xi = \int_{\psi_m}^{\psi} \frac{d\psi}{\sqrt{(a_0-\psi)(\psi-\psi_m)(\psi-\psi_l)}}$ and $2\sqrt{\frac{\alpha_4}{3}}\xi = \int_{\psi}^{\psi_l} \frac{d\psi}{\sqrt{(a_0-\psi)(\psi_m-\psi)(\psi_l-\psi)}}$. Thus, the two oval orbits give rise to two periodic solutions as follows

$$\phi(\xi) = \mp\left(\psi_l + \frac{\psi_m - \psi_l}{\mathrm{dn}^2(\Omega_9\xi, k)}\right)^{\frac{1}{2}}, \tag{41}$$

where $k^2 = \frac{a_0-\psi_m}{a_0-\psi_l}, \Omega_9 = \sqrt{\frac{\alpha_4(a_0-\psi_l)}{3}}$. The two open orbits give rise to two compacton solutions as follows

$$\phi(\xi) = \mp\left(\psi_m - \frac{\psi_m - \psi_l}{\mathrm{cn}^2(\Omega_9\xi, k)}\right)^{\frac{1}{2}}, \quad \xi \in (-\xi_{11}, \xi_{11}), \tag{42}$$

where $k^2 = \frac{a_0-\psi_m}{a_0-\psi_l}, \xi_{11} = \frac{1}{\Omega_9}\mathrm{cn}^{-1}\sqrt{1-\frac{\psi_l}{\psi_m}}$.

(10) Consider the phase portrait in Fig.2 (k).

The level curves defined by $H_1(\phi,y)=h_3$ contain two homoclinic orbits to the equilibrium points $E_{3\mp}(\mp\phi_3,0)$, respectively, and two open orbits which tend to the singular straight line $\phi=0$, respectively, when $|y|\to\infty$. In this case, (16) can be written as $2\sqrt{\frac{\alpha_4}{3}}\xi=\int_{\psi_m}^{\psi}\frac{(a_0-\psi)d\psi}{(\psi_3-\psi)\sqrt{(a_0-\psi)(\psi-\psi_m)(\psi-\psi_l)}}$ and $2\sqrt{\frac{\alpha_4}{3}}\xi=\int_{\psi}^{\psi_l}\frac{(a_0-\psi)d\psi}{(\psi_3-\psi)\sqrt{(a_0-\psi)(\psi_m-\psi)(\psi_l-\psi)}}$.

Two homoclinic orbits correspond to the the following two solitary wave solutions

$$\begin{aligned}\phi(\chi)&=\mp\left(\psi_l+\frac{\psi_m-\psi_l}{\mathrm{dn}^2(\chi,k)}\right)^{\frac{1}{2}},\quad \chi\in(-\chi_{07},\chi_{07}),\\ \xi(\chi)&=\sqrt{\frac{3}{\alpha_4(a_0-\psi_l)}}\left[\left(\frac{a_0-\psi_l}{\psi_3-\psi_l}\right)\chi\pm\left(\frac{(a_0-\psi_3)(\psi_m-\psi_l)}{(\psi_3-\psi_m)(\psi_3-\psi_l)}\right)\Pi(\arcsin(\mathrm{sn}(\chi,k)),\hat{\alpha}_7^2,k)\right],\end{aligned}\tag{43}$$

where $k^2=\frac{a_0-\psi_m}{a_0-\psi_l},\hat{\alpha}_7^2=\frac{k^2(\psi_3-\psi_l)}{\psi_3-\psi_m},\chi_{07}=\mathrm{dn}^{-1}\sqrt{\frac{\psi_m-\psi_l}{\psi_3-\psi_l}}$.

Two open orbits give rise to the following two compacton solutions

$$\begin{aligned}\phi(\chi)&=\mp\left(\psi_m-\frac{\psi_m-\psi_l}{\mathrm{cn}^2(\chi,k)}\right)^{\frac{1}{2}},\quad \chi\in(-\chi_{08},\chi_{08}),\\ \xi(\chi)&=\pm\sqrt{\frac{3}{\alpha_4(a_0-\psi_l)}}\left[\left(\frac{a_0-\psi_m}{\psi_3-\psi_m}\right)\chi+\left(\frac{(a_0-\psi_3)(\psi_l-\psi_m)}{(\psi_3-\psi_l)(\psi_3-\psi_m)}\right)\Pi(\arcsin(\mathrm{sn}(\chi,k)),\hat{\alpha}_8^2,k)\right],\end{aligned}\tag{44}$$

where $k^2=\frac{a_0-\psi_m}{a_0-\psi_l},\hat{\alpha}_8^2=\frac{\psi_3-\psi_m}{\psi_3-\psi_l},\chi_{08}=\mathrm{cn}^{-1}\sqrt{1-\frac{\psi_l}{\psi_m}}$.

(11) Consider the phase portrait in Fig.2 (l).

The level curves defined by $H_1(\phi,y)=h_1=h_3$ contain two heteroclinic orbit loops connecting the equilibrium points $E_{1\mp}(\mp\phi_1,0)$ and $E_{3\mp}(\mp\phi_3,0)$, respectively. In this case, (16) can be written as $2\sqrt{\frac{\alpha_4}{3}}\xi=\int_{\psi_2}^{\psi}\frac{(a_0-\psi)d\psi}{(\psi_3-\psi)(\psi-\psi_1)\sqrt{a_0-\psi}}$. Hence, it gives rise to the following kink and anti-kink wave solutions

$$\begin{aligned}\phi(\chi)&=\mp(\psi(\chi))^{\frac{1}{2}}=\mp\left(a_0-(a_0-\psi_1)\tanh^2\left(\tfrac{1}{2}\sqrt{a_0-\psi_1}\chi-\chi_{09}\right)\right)^{\frac{1}{2}},\\ \xi(\chi)&=\sqrt{\frac{3}{\alpha_4}}\left[\chi\pm\left(\frac{2}{\psi_3-\psi_1}\right)\left(\frac{\tanh^{-1}\sqrt{\frac{a_0-\psi(\chi)}{a_0-\psi_1}}}{\sqrt{a_0-\psi_1}}-\frac{\tanh^{-1}\sqrt{\frac{a_0-\psi(\chi)}{a_0-\psi_3}}}{\sqrt{a_0-\psi_3}}-A_0\right)\right],\end{aligned}\tag{45}$$

where $\chi_{09}=\tanh^{-1}\sqrt{\frac{a_0-\psi_2}{a_0-\psi_1}},A_0=\frac{\tanh^{-1}\sqrt{\frac{a_0-\psi_2}{a_0-\psi_1}}}{\sqrt{a_0-\psi_1}}-\frac{\tanh^{-1}\sqrt{\frac{a_0-\psi_2}{a_0-\psi_3}}}{\sqrt{a_0-\psi_3}}$.

(12) Consider the phase portrait in Fig.2 (m).

The level curves defined by $H_1(\phi,y)=h_1$ contain two homoclinic orbits to the equilibrium points $E_{1\mp}(\mp\phi_1,0)$, respectively, and two open orbits which tend to two singular straight lines $\phi=\mp\sqrt{a_0}$, respectively, when $|y|\to\infty$. In

this case, (16) can be written as $2\sqrt{\frac{\alpha_4}{3}}\xi = \int_{\psi}^{\psi_M} \frac{(a_0-\psi)d\psi}{(\psi-\psi_1)\sqrt{(a_0-\psi)(\psi_L-\psi)(\psi_M-\psi)}}$ and $2\sqrt{\frac{\alpha_4}{3}}\xi = \int_{\psi_L}^{\psi} \frac{(a_0-\psi)d\psi}{(\psi-\psi_1)\sqrt{(a_0-\psi)(\psi-\psi_L)(\psi-\psi_M)}}$.

The two homoclinic orbits give rise to two solitary wave solutions as follows

$$\begin{aligned}
&\phi(\xi) = \mp\left(\psi_L - \frac{\psi_L-\psi_M}{\mathrm{cn}^2(\chi,k)}\right)^{\frac{1}{2}}, \quad \chi \in (-\chi_{10}, \chi_{10}),\\
&\xi(\chi) = \sqrt{\frac{3}{\alpha_4(a_0-\psi_M)}}\left[\left(\frac{a_0-\psi_L}{\psi_L-\psi_1}\right)\chi \pm \left(\frac{(\psi_L-\psi_L)(a_0-\psi_1)}{(\psi_L-\psi_1)(\psi_M-\psi_1)}\right)\Pi(\arcsin(\mathrm{sn}(\chi,k), \hat{\alpha}_9^2, k)\right],
\end{aligned} \tag{46}$$

where $k^2 = \frac{a_0-\psi_L}{a_0-\psi_M}, \hat{\alpha}_9^2 = \frac{\psi_L-\psi_1}{\psi_M-\psi_1}, \chi_{10} = \mathrm{cn}^{-1}\sqrt{\frac{\psi_L-\psi_M}{\psi_L-\psi_1}}$. The two open orbits give rise to two compacton solutions as follows

$$\begin{aligned}
&\phi(\xi) = \mp\left(\psi_M + \frac{\psi_L-\psi_M}{\mathrm{dn}^2(\chi,k)}\right)^{\frac{1}{2}}, \quad \chi \in (-\chi_{11}, \chi_{11}),\\
&\xi(\chi) = \sqrt{\frac{3}{\alpha_4(a_0-\psi_M)}}\left[\left(\frac{a_0-\psi_M}{\psi_M-\psi_1}\right)\chi - \left(\frac{(a_0-\psi_1)(\psi_M-\psi_L)}{(\psi_L-\psi_1)(\psi_M-\psi_1)}\right)\Pi(\arcsin(\mathrm{sn}(\chi,k), \hat{\alpha}_{10}^2, k)\right],
\end{aligned} \tag{47}$$

where $k^2 = \frac{a_0-\psi_L}{a_0-\psi_M}, \hat{\alpha}_{10}^2 = \frac{k^2(\psi_M-\psi_1)}{\psi_L-\psi_1}, \chi_{11} = \mathrm{dn}^{-1}\sqrt{\frac{\psi_L-\psi_M}{a_0-\psi_M}}$.

5 Conclusion

The results of the above analysis and discussion can be formulated in the following theorem.

Theorem 1 *For the parameters of equation (2), we write that* $a_0 = \frac{a}{3\theta_1+\theta_2+\theta_3}, \beta = \frac{3\theta_1+\theta_2+\theta_3}{6\theta_1}, g_0 = \frac{-b_1}{6\theta_1} \neq 0, \alpha_0 = \frac{a_1}{6\theta_1}, \alpha_2 = -\frac{a_3}{6\theta_1}, \alpha_4 = -\frac{b_3}{6\theta_1}$ *and assume that* $a_0\alpha_0\alpha_2\alpha_4 g_0\theta_1 \neq 0$. *Then, the following conclusions hold.*

(i) Equation (2) has the exact explicit solutions with the form $q(x,t) = \phi(\xi)\exp(i(-kx+\omega t)), \xi = x - \nu t$, *where* $\phi(\xi)$ *is an exact solution of the singular traveling wave system (6).*

(ii) Assume that $3\theta_1 = \theta_2 + \theta_3$. *Then, when* $\Delta > \alpha_2^2 - 4\alpha_0\alpha_4 > 0, \alpha_0 < 0, \alpha_4 > 0, 0 < g_0 < |g_e^*|$, *system (6) has the bifurcations of phase portraits which are shown in Fig.1, while* $\Delta > 0$ *and* $\alpha_0\alpha_4 > 0, \alpha_2 < 0, \alpha_4 > 0, -g^* < g_0 < 0$, *system (6) has the bifurcations of phase portraits which are shown in Fig.2, where* g_e^* *and* g^* *is defined by (14).*

(iii) System (6) has exact explicit solitary wave solutions given by (21), (23), (25), (27), (35), (43), (46).

(iv) System (6) has exact explicit pseudo-peakon solutions given by (24), (38).

(v) System (6) has exact explicit peakon and anti-peakon solutions given by (20), (26), (36).

(vi) System (6) has exact explicit periodic wave solutions given by (29), (31).

(vii) System (6) has exact explicit periodic peakon solutions given by (17), (18), (22), (32), (33), (37).

(viii) System (6) has exact explicit compacton solutions given by (19), (28), (30), (34), (39), (40), (44), (47).

(ix) System (6) has exact explicit kink and anti kink wave solutions given by (45).

In summary, this paper study Raman soliton model in nanoscale optical waveguides, having anti-cubic nonlinearity. Under different parameter conditions, we obtain variety of exact solutions such as solitary wave solutions, periodic wave solutions, periodic peakons and peakons, compacton solutions etc. via bifurcation theory of dynamical system. We can see that the solutions of the system (6) have very abounded dynamical behaviors. Compared to the results in [4], our work extends the results in the following aspects. Firstly, we present all types of traveling wave solutions and give their exact explicit parametric representations, while the only solitary and periodic wave solutions were shown in [4]. Secondly, the solutions in [4] were obtained under specific parameter condition, while we consider the dynamical behaviors of the traveling wave solutions under general parameters conditions. Additionally, these abundant dynamic behaviors of solutions are helpful for us to understand some phenomena in optical waveguides and have the potential to contribute on the applications of non-linear optics.

Acknowledgements This research was partially supported by the National Natural Science Foundation of China (11371326, 11975145, 11871231, 12071162, 11701191, 11901215).

Compliance with ethical standards

Conflict of interest

The authors declare that they have no conflict of interest.

Data availability statements

The authors declare that all data generated or analysed during this study are available within the article and its supplementary information files.

References

1. Xu, Y., Pablo Suarez, P., Milovic, D., Khan, K. R., Mahmood, M. F., Biswas, A., Belic, M.: Raman solitons in nanoscale optical waveguides, with metamaterials, having polynomial law nonlinearity, J. of Modern Optics, **63:53**(2016), 532-537.
2. Xiang, Y., Dai, X., Wen, S., Guo, J., Fan, D.: Controllable Raman soliton self-frequencyshift in nonlinear metamaterials, Phys. Rev. A, **84**(2011), 033815.
3. Zhou, Y., Li, J.: Exact solutions and dynamics of the Raman soliton model in nanoscale optical waveguides, with metamaterials, having polynomial law nonlinearity, Int. J. of Bifurcation and Chaos, **27:12**(2017), 1750188.

4. Al-Ghafri, K.S., Krishnan, E.V.:Optical solitons in metamaterials dominated by anti-cubic nonlinearity and hamiltonian perturbations,Int. J. Appl. Comput. Math.,**6**(2020),144.
5. Foroutan, M., Manafian, J., Ranjbaran, A.: Solitons in optical metamaterials with anti-cubic law of nonlinearity by generalized $\frac{G'}{G}$-expansion method, Optik, **162**(2018), 86.
6. Ekici, M., Sonmezoglu, A., Zhou, Q., Moshokoa, S.P., Ullah, M.Z., Arnous, A.H., Biswas, A., Belic, M.: Analysis of optical solitons in nonlinear negative-indexed materials with anti-cubic nonlinearity, Opt. Quantum Electron, **50**(2018), 75.
7. Foroutan, M., Manafian, J., Zamanpour, I.: Solitonwave solutions in optical metamaterials with anti-cubic law of nonlinearity by ITEM, Optik, **164**(2018), 371.
8. Biswas, A., Ekici, M., Sonmezoglu, A., Zhou, Q., Alshomrani, A. S., Moshokoa, S. P., Belic, M.: Solitons in optical metamaterials with anti-cubic nonlinearity, Eur. Phys. J. Plus, **133**(2018), 204.
9. Kader, A. A., Latif, M. A., Zhou, Q.: Exact optical solitons in metamaterials with anti-cubic law of nonlinearity by Lie group method, Opt. Quantum Electron, **51**(2019), 30.
10. Al-Ghafri, K.S.: Solitary wave solutions of two KdV-type equations, Open Phys., **16**(2018), 311-318.
11. Zayed, E., Alurrfi, K.: New extended auxiliary equation method and its applications to nonlinear Schrodinger-type equations, Optik, **127**(2016), 9131.
12. Zeng, X.,Yong, X.: Anewmapping method and its applications to nonlinear partial differential equations, Phys. Lett. A, **372**(2008), 6602.
13. Zheng, B.: A new Bernoulli sub-ODE method for constructing traveling wave solutions for two nonlinear equations with any order, U. Politeh. Buch. Ser. A, **73**(2011), 85.
14. Li, J., Chen, G.: Bifurcations of travelling wave solutions for four classes of nonlinear wave equations, Int. J. Bifurcation and Chaos, **15:9**(2005), 2913-2926.
15. Li, J., Chen, G.: On a class of singular nonlinear traveling wave equations, Int. J. Bifurcation and Chaos, **17:11**(2007), 4049-4065.
16. Li, J.: Singular Nonlinear Traveling Wave Equations: Bifurcations and Exact Solutions, Science Press, Beijing, 2013.
17. Li, J., Zhou, W., Chen, G.: Understanding peakons, periodic peakons and compactons via a shallow water wave equation, Int. J. Bifurcation and Chaos, **26:12**(2016), 1650207.
18. Li, J., Zhang, Y., Zhao, X.: On a class of singular nonlinear traveling wave equations (II): an example of GCKdV equations, Int. J. Bifurcation and Chaos, **19**(2009), 1955-2007.
19. Biswas, A., Mirzazadeh, A., Savescu, M., Milovic, D., Khan, K. R., Mahmood, M. F. & Belich, M.: Singular solitons in optical metamaterials by ansatz method and simplest equation approach, J. of Modern Optics, **61:19**(2014), 1550-1555.
20. Biswas, A., Kaisar R. Khan, K. R., Mahmood, M. F. & Belic, M.: Bright and dark solitons in optical metamaterials, Optik, **125**(2014), 3299-3302.
21. Byrd, P.F. & Fridman, M.D.: Handbook of Elliptic Integrals for Engineers and Sciensists, Springer, Berlin, 1971.
22. Sonmezoglu, A., Yao, M., Ekici, M., Mirzazadeh, M. and Zhou, Q.: Explicit solitons in the parabolic law nonlinear negative-index materials, Nonlinear Dyn., **88**(2017), 595-607.
23. Zhou, Q., Liu, L., Liu, Y.,Yu, H., Yao, P., Wei, C., Zhang, H.: Exact optical solitons in metamaterials with cubic-quintic nonlinearity and third-order dispersion, Nonlinear Dyn., **80**(2015), 1365-1371.
24. Zhou, Q., Mirzazadeh, M., Ekici, M., Sonmezoglu, A.: Analytical study of solitons in non-Kerr nonlinear negative index materials, Nonlinear Dyn., **86**(2015), 623-638.

Figures

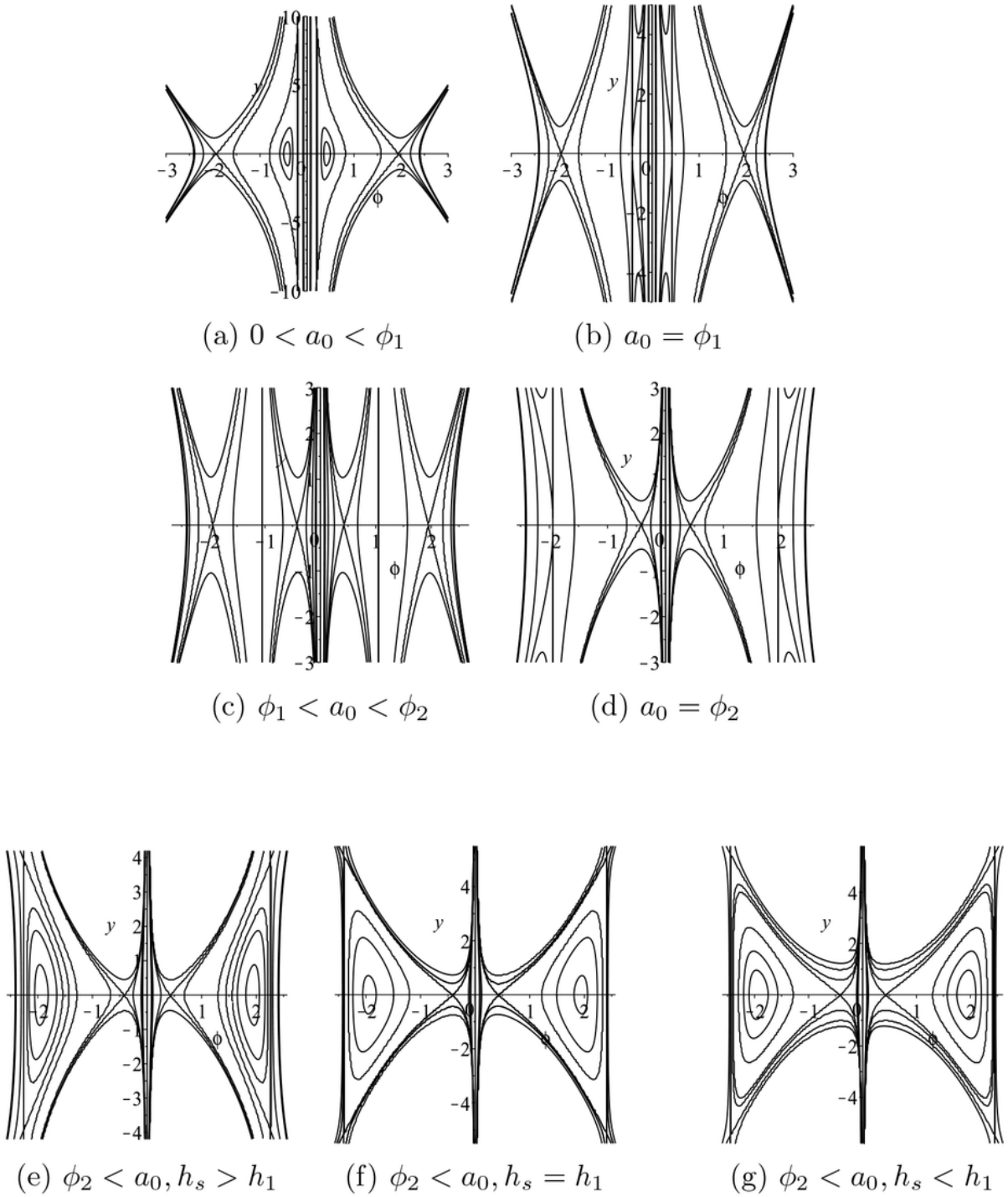

Figure 1

The bifurcations of phase portraits of system (6) when F(Φ) has four zeros

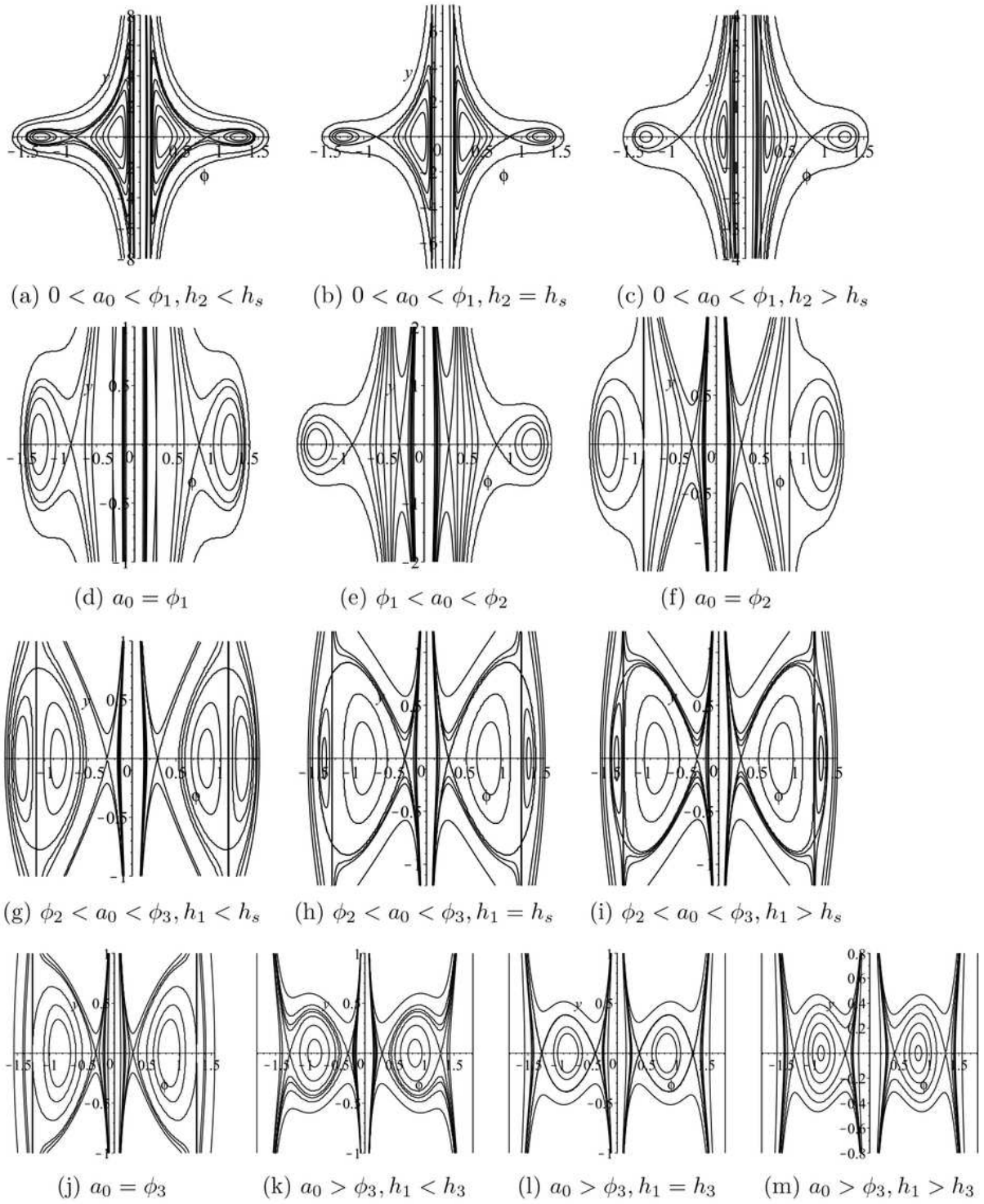

Figure 2

The bifurcations of phase portraits of system (6) when F(Φ) has six zeros

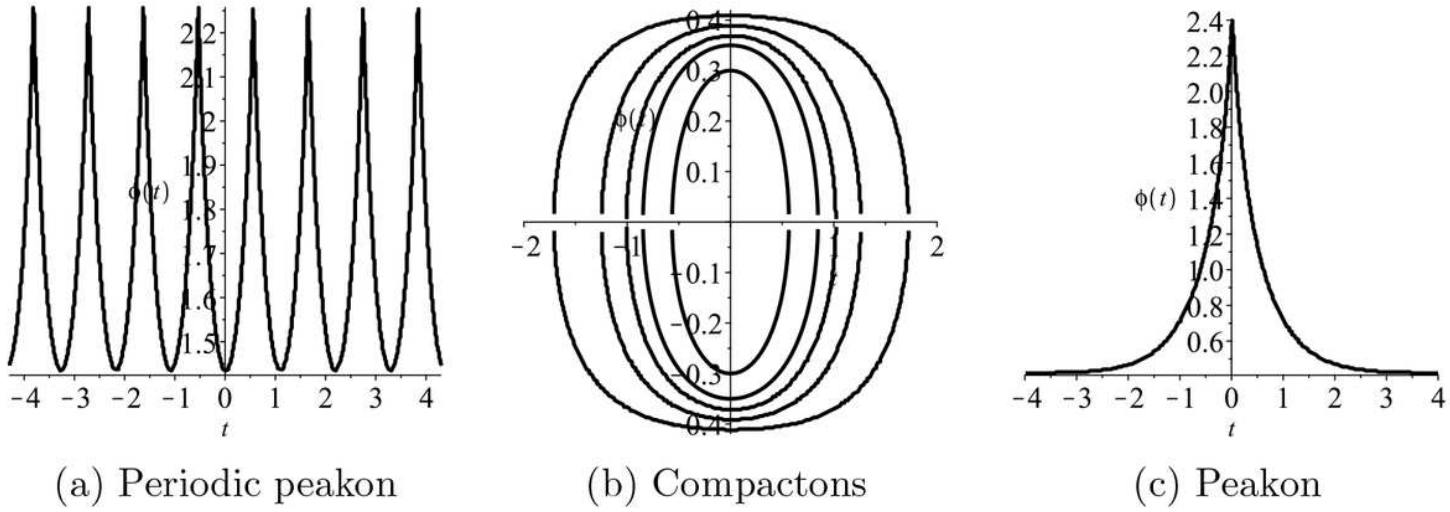

Figure 3

The profiles of periodic peakon, compactons and peakon of system (6)

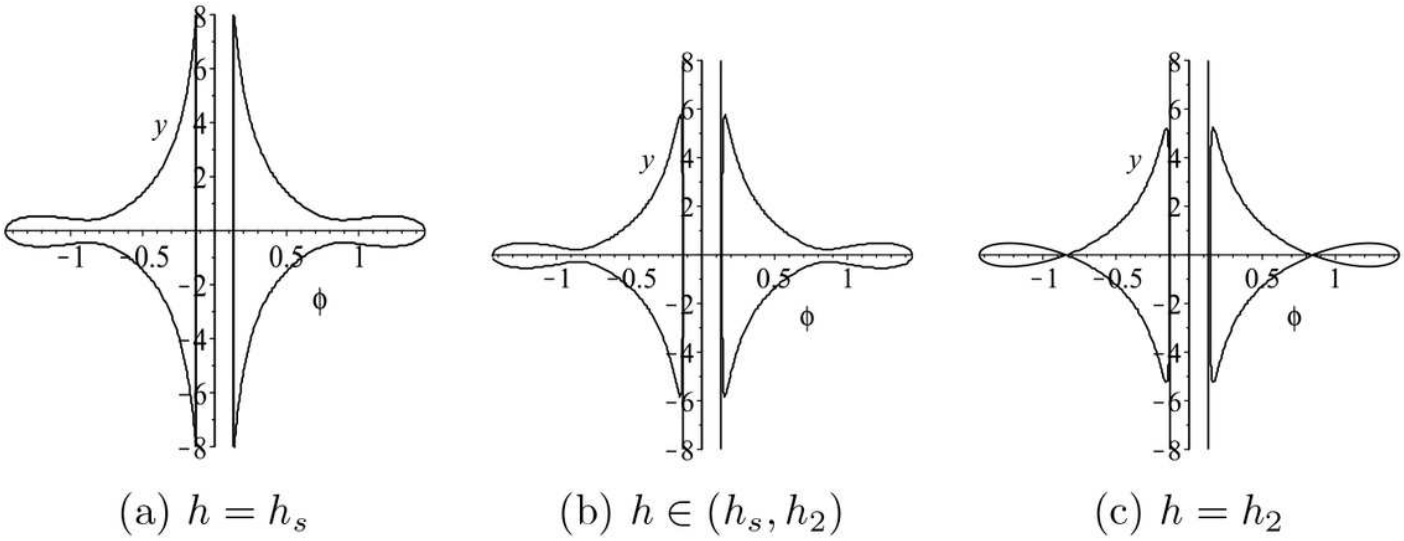

Figure 4

The level curves defined by H1(Φ, y) = h of system (6) in Fig.2 (a)

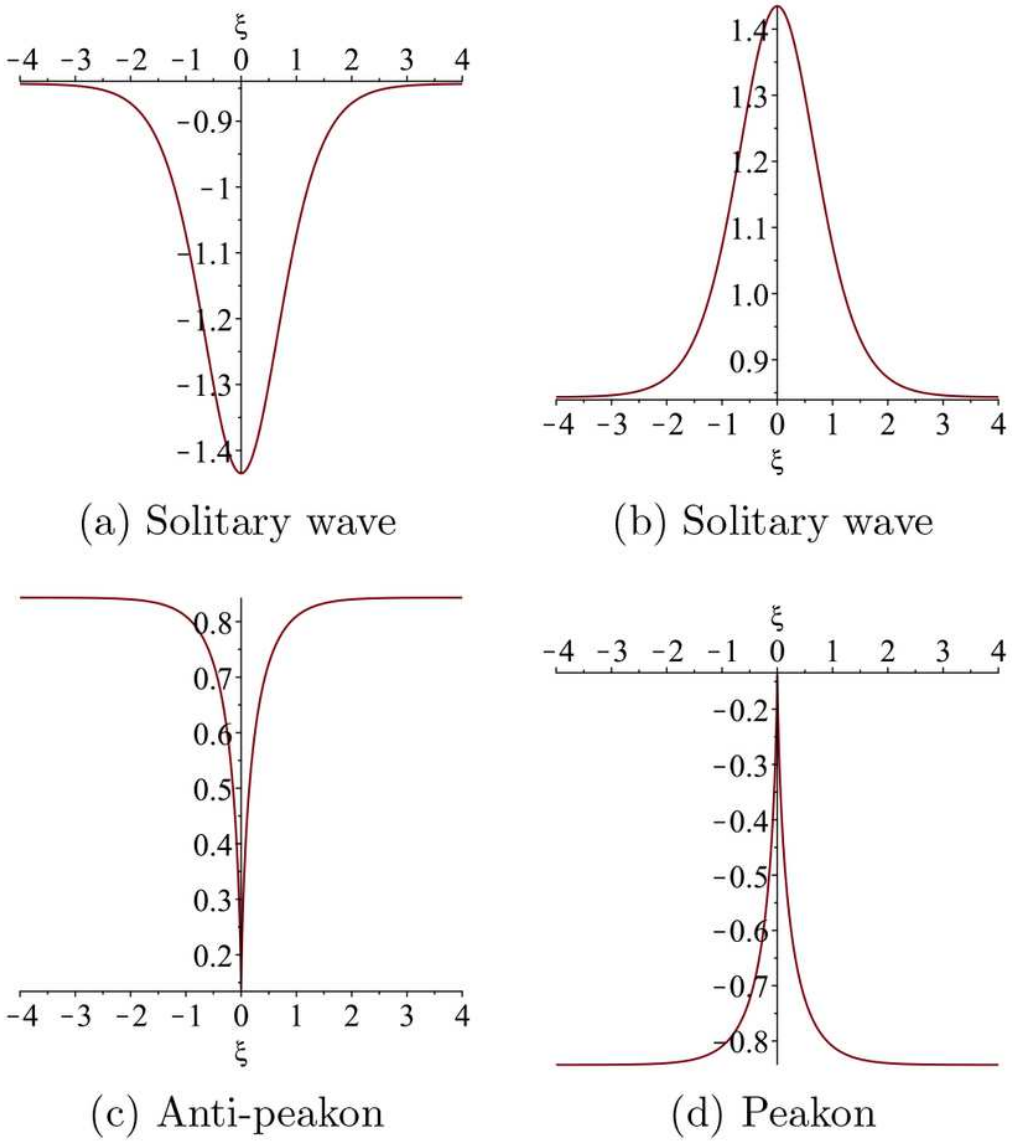

Figure 5

The profiles of solitary waves and peakon, anti-peakon of system (6) given by (25), (26)

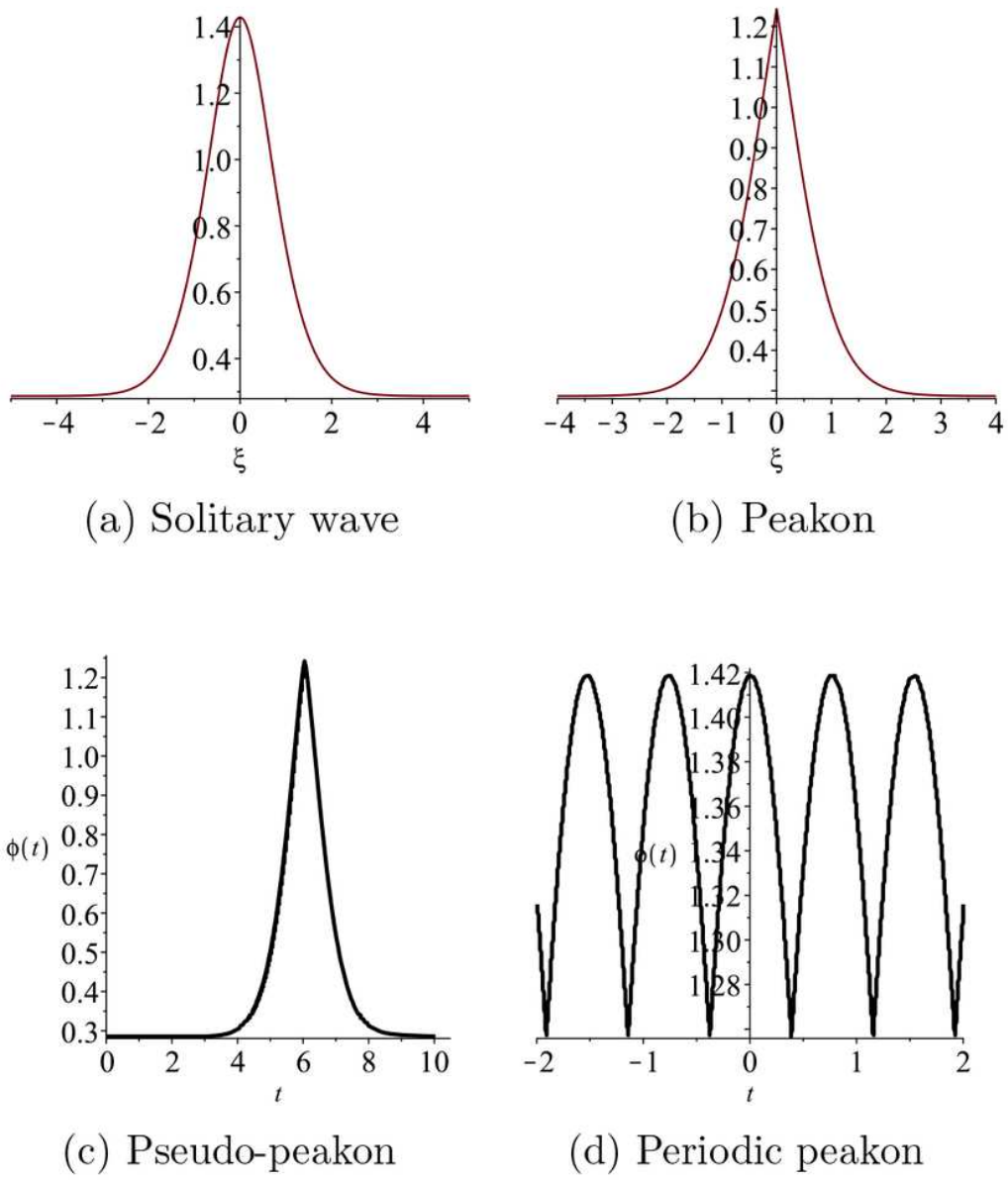

Figure 6

The profiles of solitary wave, pseudo-peakon, peakon and periodic peakon of system (6)